Journal of
Molluscan Studies

The Malacological Society of London

Journal of Molluscan Studies (2014) **80**: 8–16. doi:10.1093/mollus/eyt044

EMBRYONIC AND LARVAL DEVELOPMENT OF *RUDITAPES DECUSSATUS* (BIVALVIA: VENERIDAE): A STUDY OF THE SHELL DIFFERENTIATION PROCESS

JOSE ANDRÉS ARANDA-BURGOS[1], FIZ DA COSTA[1,2], SUSANA NÓVOA[1], JUSTA OJEA[1] AND DOROTEA MARTÍNEZ-PATIÑO[1]

[1]*Centro de Investigacións Mariñas, Consellería do Mar, Xunta de Galicia, Muelle de Porcillán s/n, 27700 Ribadeo, Lugo, Spain; and*
[2]*Present address: Ifremer, Laboratoire de Physiologie des Invertébrés Marins, Station Expérimentale d'Argenton, Presqu'ile du Vivier, 29840 Landunvez, France*

Correspondence: F. da Costa; e-mail: fiz.da.costa.gonzalez@ifremer.fr

(Received 3 August 2012; accepted 25 July 2013)

ABSTRACT

The embryonic and larval development of *Ruditapes decussatus*, from fertilization to metamorphosis, is described using scanning electron microscopy (SEM). Shell formation during embryonic development is investigated using SEM and transmission electron microscopy (TEM). Released oocytes are about 67 μm in diameter. Gastrulation takes place by epiboly and starts 7 h after fertilization ($T_0 + 7$ h). The early gastrula is characterized by the appearance of a large, open cavity posteriorly and a small, round blastopore anteriorly, which represent the shell field and the blastopore, respectively. In TEM views, the open cavity expands under and posterior to the developing prototrochal pad. The shell field comprises a few cells in which microvilli progressively regress; these cells will secrete the periostracum. After 13 h ($T_0 + 13$ h) the late gastrula has differentiated into a typically pyriform and motile trochophore. The periostracum emerges from periostracum-secreting cells (T1) and spreads over shell-secretory cells (T3). Thus, the trochophore is laterally compressed and the periostracum inserts to the mantle edge. Typical straight-hinged D-shaped larvae develop from a trochophore by 26 h postfertilization ($T_0 +$ 26 h) and by then the valves completely enclose the soft body of the larva. At $T_0 + 39$ h, the newly hatched veliger larva is already enclosed in the fully calcified prodissoconch I (PI) and the prototroch has transformed into the velum. Late D-larvae already have a developed digestive system and start exogenous feeding. At the same time, the prodissoconch II is newly secreted at the margin of the PI. Settlement occurs at 27 d postfertilization ($T_0 + 27$ d), when the larvae are about 207 μm long. Once metamorphosis is completed, the mantle folds begin the secretion of the dissoconch shell and the postlarval stage is reached.

INTRODUCTION

The grooved carpet shell *Ruditapes decussatus* (Linnaeus, 1758) is distributed from the North Sea to Senegal and through the Mediterranean Sea, where it lives buried or partly buried in sand or mud, mainly in the intertidal zone, although it also inhabits subtidal zones (Vela & Moreno, 2005).

Larval development has been described in several species of Eulamellibranchia, providing basic knowledge for aquaculture and for identification of larval stages in the plankton (Loosanoff & Davis, 1963; Loosanoff, Davies & Chanley, 1966). Various aspects of embryonic and larval development have been described in numerous species using light and scanning electron microscopy (SEM) (e.g. Bellolio, Lohrmann & Dupre, 1993; Gros, Duplessis, & Felbeck, 1999; Mouëza, Gros & Frenkiel, 1999), however investigations using transmission electron microscopy (TEM) are scarce (e.g. Eyster & Morse, 1984; Mouëza, Gros & Frenkiel, 2006).

Although various aspects of larval morphology have been investigated in previous studies, differentiation process of the shell field and the structure of the earliest formed shell are among the most poorly known aspects of bivalve larval morphology (Bellolio, Lohrmann & Dupre, 1993; Weiss *et al.*, 2002; Cragg, 2006). In molluscs, shell formation is initiated during embryogenesis. In bivalves, the larval shell is called the prodissoconch and it is composed of two distinct regions: prodissoconch I (PI) and prodissoconch II (PII) (Ockelmann, 1965). It is generally accepted that the secretion of the very first shell material by shell-field epithelial cells is preceded by an invagination of the dorsal ectoderm region of the shell field (Eyster & Morse, 1984). During gastrulation, two independent depressions are observed, the smaller being the blastopore and the larger the shell field.

The first observations of the differentiation of the shell field during embryonic development were made in gastropods by Gegenbaur and in bivalves by Stepanoff (in Kniprath, 1980). Early shell-field formation in *Mytilus edulis* was investigated with TEM by Kniprath (1980), who suggested that the invagination needs to close before shell formation. A few years later, Eyster & Morse (1984) in *Spisula solidissima*, and Casse, Devauchelle & Le Pennec (1998) in *Pecten maximus*, confirmed this theory. However, Mouëza, Gros & Frenkiel (2006), studying *Chione cancellata*, proposed an alternative interpretation of shell differentiation in bivalves, in which the shell field did not migrate inward and never formed an invagination. The prototrochal pad and the shell field constituted an open cavity, at the far end of which they were in close contact. These authors also described the cell types involved in shell secretion, which were: T1 cells or periostracum-secretory cells, and T3 cells or nonperiostracum-secretory cells, which were involved in the production of the second organic layer of the shell and in shell calcification.

A variety of types of larval development occur in the Bivalvia (Chanley, 1968). In marine bivalves, the most common developmental pattern is the release of gametes to the sea water, and consequently fertilization and embryonic development occur externally (Ockelmann, 1965). The resulting larva is a mobile ciliated trochophore, which upon secretion of the PI becomes the planktonic D-veliger larva. Further secretion at the rim of the D-shaped prodissoconch shell produces the PII. During early development, the prototroch of the trochophore becomes the rim of the velum of the veliger larva. When the larva becomes capable of crawling as well as swimming, it reaches the pediveliger stage which heralds metamorphosis (Cragg & Crisp, 1991).

The appearance of a pelagic larva in the life cycle of most marine bivalve molluscs is accompanied by anatomical adaptations, especially those associated with the velum. The velum is an adaptation for planktonic life (Cragg, 1989) and emerges as a distinct organ in the early veliger stage of bivalve development, disappearing when the pediveliger metamorphoses. The composition of the ciliary bands on the velum has been described with electron microscopy in other bivalves (e.g. Cragg, 1989; Chaparro, Thompson & Emerson, 1999). These authors agreed on the presence of at least three bands of cilia: an inner preoral band, an adoral band and an outer postoral band. The inner preoral band is closest to the upper velar surface and consists of a group of longer cilia. Below this, there is a band of smaller cilia, the adoral band. Finally, on the part of the velum closest to the shell, there is a single line of cilia, similar in size to the adoral band, which is the postoral band.

This is the first study on the embryology and larval development of *R. decussatus*, with special reference to the shell differentiation process using SEM and TEM. The aims of this study were (1) to test if the shell differentiation model proposed by Mouëza, Gros & Frenkiel (2006) for *C. cancellata* is also valid in other venerids and (2) to provide a detailed description of the external embryo and larval morphology of *R. decussatus* with SEM.

MATERIAL AND METHODS

Spawning induction and fertilization

Adult specimens of *Ruditapes decussatus* were collected by rake in March 2009 in a natural bed in the intertidal zone at Cambados in Ría de Arousa (Galicia, NW Spain). Clams were transferred, while cooled at 4°C, to our hatchery facilities. At Centro de Cultivos de Ribadeo-CIMA, broodstock clams were conditioned at 18 ± 1°C in open-circuit aquaria, with a continuous supply of a mixture of *Isochrysis galbana*, *Pavlova lutheri*, *Tetraselmis suecica*, *Chaetoceros* sp. and *Skeletonema marinoi*.

For spawning induction, 79 individuals were cleaned and kept dry at 4°C for 12 h. Then, clams were placed in a tray with UV-sterilized seawater. Thermal shock (temperature rise from 14 to 25°C) with addition of microalgae and gonad extracts was carried out to induce spawning. Each spawning specimen was quickly transferred into an individual receptacle for the release of sperm or eggs, thus avoiding self-fertilization. Once spawning was completed, sperm from several males was pooled and added to the container, at 20 ± 1°C, with oocytes to obtain synchronous fertilization. After fertilization, the eggs were sieved through a 45-μm mesh to eliminate excess sperm.

Larval culture

Embryos were transferred to 500-l larval culture tanks with aerated water at a temperature of 20 ± 1°C. The density of the embryos was adjusted to 6.5/ml. Water was changed every 2 d using 1-μm filtered, UV-sterilized seawater. D-stage veliger larvae were fed daily with *I. galbana*, *P. lutheri*, *S. marinoi*, *Chaetoceros* sp. and *T. suecica* at 40 cells/μl as an initial ration.

Scanning electron microscopy

Samples were collected throughout embryonic development, every 10 min, from fertilized egg to trochophore, every hour from trochophore to D-larva and every day from D-larva onwards. At least 100 individuals were collected per stage of development, photographed and measured using an optical microscope. Samples were fixed at 4°C in 2.5% glutaraldehyde in 0.1 M sodium cacodylate buffer solution. After rinsing in cacodylate buffer, embryos were dehydrated in an ascending series of ethanol washes and critical-point dried using CO_2. Embryos were then sputter-coated with gold before observation in two scanning electron microscopes, a Philips XL30 and a Jeol JSM 6700.

Transmission electron microscopy

From blastula to D-larva, samples were collected and prefixed following the same procedure as for SEM. After rinsing samples in cacodylate buffer, embryos were dehydrated in an ascending series of acetone washes and embedded in Spurr resin, first at 4°C, then at room temperature and finally at 60°C for 48 h. Thin sections (70–90 nm) were cut using a Leica Reichert Ultracut and were contrasted for 30 min in 2% aqueous uranyl acetate and 10 min in 0.1% lead citrate before examination using a FIB FEI Helios 600 Nanolab and a Jeol Jem 1010 transmission electron microscope.

RESULTS

Successful spawning was obtained by keeping individuals dry at 4°C for 12 h and then subjecting them to thermal shock. Eighteen females out of a batch of 79 individuals spawned and *c.* 1.8 million eggs per female were released.

Unfertilized eggs of *Ruditapes decussatus* were spherical and had a mean diameter of 67.43 ± 3.62 μm ($n = 100$; Fig. 1A). A 1–2 μm vitelline coat was visible by optical microscopy after fertilization was performed. Sperm appeared active at least 2 h after release and were characterized by a trumpet-shaped head, slightly curved, about 8 μm long from the tip of the acrosome to the distal end of the middle piece, which appeared to contain four mitochondria (Fig. 1B). Sperm had an overall length of about 40 μm when measured from the tip of the head to the end of the tail (Fig. 1C). Fertilization occurred normally and no polyspermy was observed.

Table 1 shows the different embryonic stages of *R. decussatus* and the times at which they occurred. The first polar body

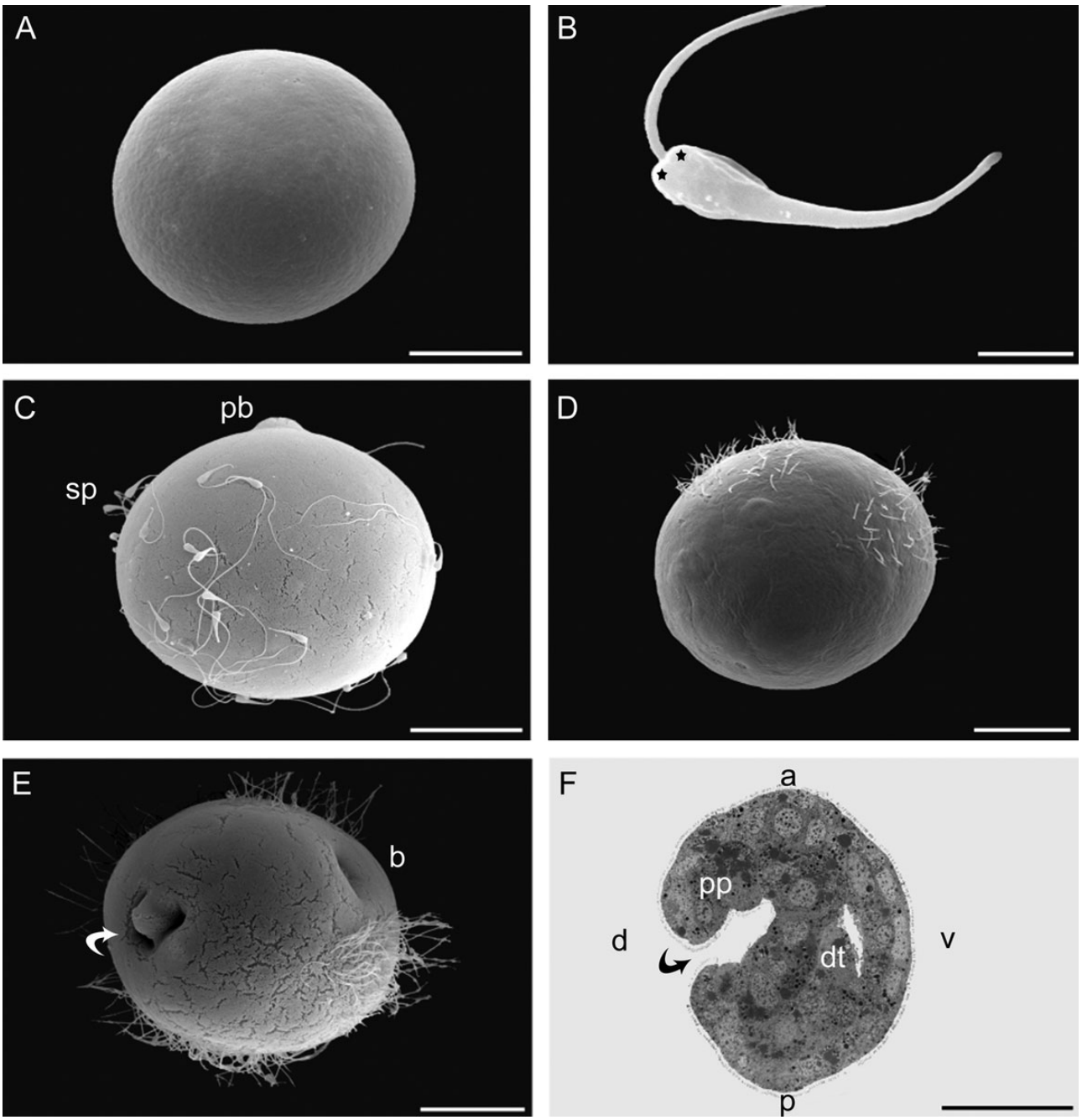

Figure 1. Development of *Ruditapes decussatus*. **A–E**. Scanning electron microphotographs. **F**. Transmission electron microphotograph. **A**. Spawned egg. **B**. Detail of sperm head, characterized by a short arched head with an elongated acrosome and middle piece with four mitochondria (asterisks). **C**. Fertilized egg showing a polar body ($T_0 + 20$ min) and sperm on its surface. **D**. Ciliated blastula showing short microvilli ($T_0 + 6$ h). **E**. Ciliated gastrula showing opening of blastopore and shell field (curved arrow) ($T_0 + 8$ h). **F**. Sagittal section of a ciliated gastrula. Abbreviations: a-p, antero-posterior axis; b, blastopore; dt, digestive tract; d-v, dorso-ventral axis; pb, polar body; pp, prototrochal pad; sp, sperm. Scale bars: **A, C–E** = 20 μm; **B** = 2 μm; **F** = 30 μm.

(Fig. 1C) appeared 20 min after fertilization ($T_0 + 20$ min) and measured *c.* 6–8 μm. The first cleavage, meridional and unequal, resulted in two unequal blastomeres. Successive cleavages produced an intermediate morula, which developed quickly into a blastula by 6 h postfertilization ($T_0 + 6$ h). This was the first motile stage in the development of the embryo and showed a few cilia on its surface (Fig. 1D). At this time a polar body, located in the plane of cleavage, was still visible. Gastrulation occurred by epiboly and started at $T_0 + 7$ h. The early gastrula stage was characterized by the appearance of two depressions: a large open cavity posteriorly and a small round blastopore anteriorly. The latter depression was originally located at the vegetal pole, but during gastrulation was displaced to the ventral side of the future larva. Moreover, some scarce cilia began to cover the anterior region of the embryo, prefiguring the future prototroch (Fig. 1E). In TEM views (Figs 1F, 2A, B), the dorsal region was marked by an open cavity, which was expanding under and posterior to the

Table 1. Embryonic and larval stages of *Ruditapes decussatus* reared at 20 ± 1°C.

Stage	Time postfertilization	Length ($n = 100$)
Unfertilized egg	0 h	67.4 ± 3.6
First polar body	20 min	
2-cell	1 h 15 min	
4-cell	1 h 45 min	
8-cell	2 h 15 min	
16-cell	4 h	
32-cell	4 h 45 min	
Blastula	6 h	
Gastrula	8 h	
Trochophore	13 h	
D-shaped larva	26 h	89.9 ± 6.5
Umbonate stage	7 d	138.7 ± 7.5
Pediveliger	15 d	180.5 ± 16.1
Metamorphosis	27 d	207.6 ± 15.4

Length in μm expressed as mean ± SD.

developing prototrochal pad. In a crosssection through the prototrochal pad and shell-field cells (Fig. 2B), the shell field was apparent, consisting of a few cells in which microvilli progressively regressed. These cells subsequently secreted the periostracum.

After 13 h ($T_0 + 13$ h) the late gastrula had differentiated into a typically pyriform and motile trochophore. The difference between the diameters of the blastopore and the other depression was obvious, and the first cilia of the future telotroch were differentiated in the posterior region (Fig. 2C). The trochophore had a crown of motile cilia, called the prototroch, which allowed active swimming and divided the trochophore into two areas. The posterior area was occupied by the blastopore on the ventral side and by the shell field on the dorsal side. The anterior pretrochal area was characterized by the long ciliary tuft of the apical sense organ. The newly secreted shell material spread out gradually and folded into right and left segments connected by a hinge line, which was clearly visible (Fig. 2F). The periostracum, which appeared as a dense pellicle under TEM (Fig. 2D, E), covered the apical poles of two adjacent shell-field cells. It emerged from secretory cells (T1) and spread over nonsecretory cells (T3). T1 cells bore a few microvilli, whereas T3 cells were devoid of microvilli (Fig. 2E). The two lobes of the saddle-shaped shell field were expanding over the body and the hinge line was well delineated (Figs 2G, 3A). Thus, the trochophore was laterally compressed and the periostracum inserted at the mantle edge (Fig. 2H).

Typical straight-hinged larvae had developed by $T_0 + 26$ h and were 89.87 ± 6.55 μm long ($n = 100$; Fig. 3B). The valves completely enclosed the soft body of the embryo and the shell gland continued the secretion of the valves. By $T_0 + 39$ h, the newly hatched veliger larva was already enclosed in the calcified PI (Fig. 3A–E). At this stage the prototroch had transformed into the velum, the oval locomotory and feeding organ of the larva.

Apart from the apical tuft, the central and upper surface of the velum was devoid of cilia (Fig. 3E). The apical tuft is a group of cirri, characteristic of planktonic veligers and measured about 80–100 μm long in the pediveliger stage (Figs 2F, 3E, 4B). The rim of the velum bore four concentric bands of cilia. The inner preoral ring consisted of a single line of a few simple cilia, each one about 10–15 μm long. The inner preoral ring and the next closest ring of preoral cirri were separated by a space. The preoral cirri formed a band of several rows of cirri. This was the most visible ring in the velum because of its width and the size and complexity of its cirri. Each cirrus was about 50–70 μm long. Below the band of preoral cirri there was a band of smaller cilia (10–20 μm), the adoral band. Finally, below this, on the part of the velum closest to the shell, there was a single line of cilia, of similar size to the adoral band, which is called the postoral band (Fig. 3D).

The late D-larvae already had a developed digestive system and were planktotrophic. At the same time, the PII was newly secreted at the margin of the PI. The PI had a smooth outer surface with a punctate pattern and measured up to 70–80 μm in diameter. The PII had an outer surface showing commarginal growth lines. There was a sharply defined transition between the two shell zones (Figs 3F, 4A). Five days after fertilization ($T_0 + 5$ d) the shell started to become oval in shape and the umbo was forming (Fig. 3F). After 7 d the larvae reached the umbonate stage, with a length of 138.73 ± 7.55 μm ($n = 100$). Fifteen-day-old larvae ($T_0 + 15$ d), which showed a still-functional velum with the apical tuft and a ciliated foot, reached the pediveliger stage (Fig. 4B, C) with a mean valve length of 180.47 ± 16.10 μm ($n = 100$). During this stage, the larva was able to crawl and swim for short intervals. After 29 d the PII had enlarged to 110–130 μm in diameter (Fig. 4D). Settlement occurred at 27 d postfertilization ($T_0 + 27$ d), at a size of 207.6 ± 15.4 μm ($n = 100$). During metamorphosis, the velum was shed completely as one unit and the gill rudiments underwent rapid histogenesis to develop into the adult gills. Once metamorphosis was complete, the mantle folds began secretion of the dissoconch shell and the postlarval stage was reached (Fig. 4D).

DISCUSSION

This study provides the first high-magnification image of the mature spermatozoon of *Ruditapes decussatus*. It is characterized by a trumpet-shaped head, which is slightly curved, and an elongated acrosome. The head morphology is different from those described in other venerid species, such as *Gafrarium tumidum*, *Circe scripta*, *Pitar sulfureum* and *Gomphina aequilatera* (Gwo *et al.*, 2002), *Chione cancellata* (Mouëza, Gros & Frenkiel, 2006) and *Venerupis pullastra* (Cerviño-Otero, 2011), but is similar to the sperm head of the lucinid *Codakia orbicularis* (Mouëza & Frenkiel, 1995). However, the curved head of the spermatozoa is a common feature in *G. tumidum*, *C. scripta*, *P. sulfureum*, *G. aequilatera* and *C. cancellata* (Gwo *et al.*, 2002; Mouëza, Gros & Frenkiel, 2006), while spermatozoa of *V. pullastra* have a straight head (Cerviño-Otero, 2011). This elongated head represents a modification of the ancestral type of spermatozoon, in which the head consists of a rounded or conical nucleus surmounted by a small acrosome (Franzen, 1955, 1956).

As occurs in other bivalves, such as *Ensis* (da Costa, Darriba & Martinez-Patino, 2008), *Spisula*, *Crassostrea*, *Mytilus*, *Pecten*, *Teredo*, *Venus* (Verdonk & van den Biggelaar, 1983) and *Venerupis* (Cerviño-Otero, 2011), in *Ruditapes* gastrulation occurs by epiboly, during which two different depressions appear, the blastopore and an open cavity. As described by Mouëza, Gros & Frenkiel (1999, 2006) and Silberfeld & Gros (2006), who studied small venerids, in *R. decussatus* the cavity of the shell gland appears when the gastrula bears only few cilia. With the sequential sampling used in this study, it has been confirmed that the differentiation of the shell gland in *R. decussatus* takes place in the gastrula stage prior to the complete formation of the prototroch. Nevertheless, there is some disagreement in the literature regarding the appearance of these two structures; for example, Eyster & Morse (1984) reported the appearance of the shell gland at a later stage in the early trochophore of *Spisula solidissima*.

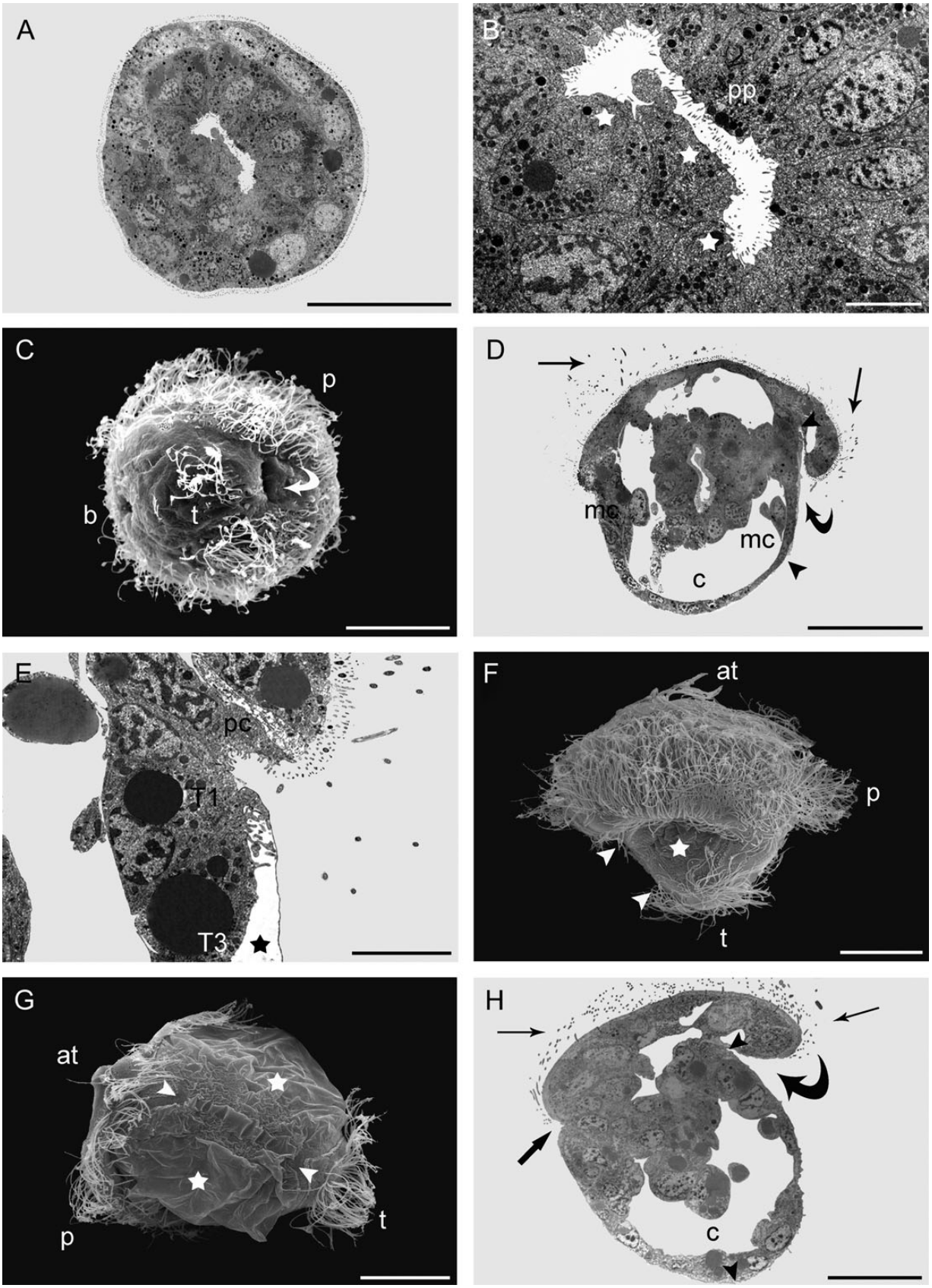

Figure 2. Development of *Ruditapes decussatus*. **C, F, G**. Scanning electron microphotographs. **A, B, D, E, H**. Transmission electron microphotographs. **A**. Cross-section of a late gastrula through shell gland invagination. **B**. Detail of figure **A** showing the prototrochal pad and shell-field cells (stars). **C**. Basal view of early trochophore showing shell-field depression (curved arrow), blastopore, telotroch and prototroch. **D**. Transverse section of a

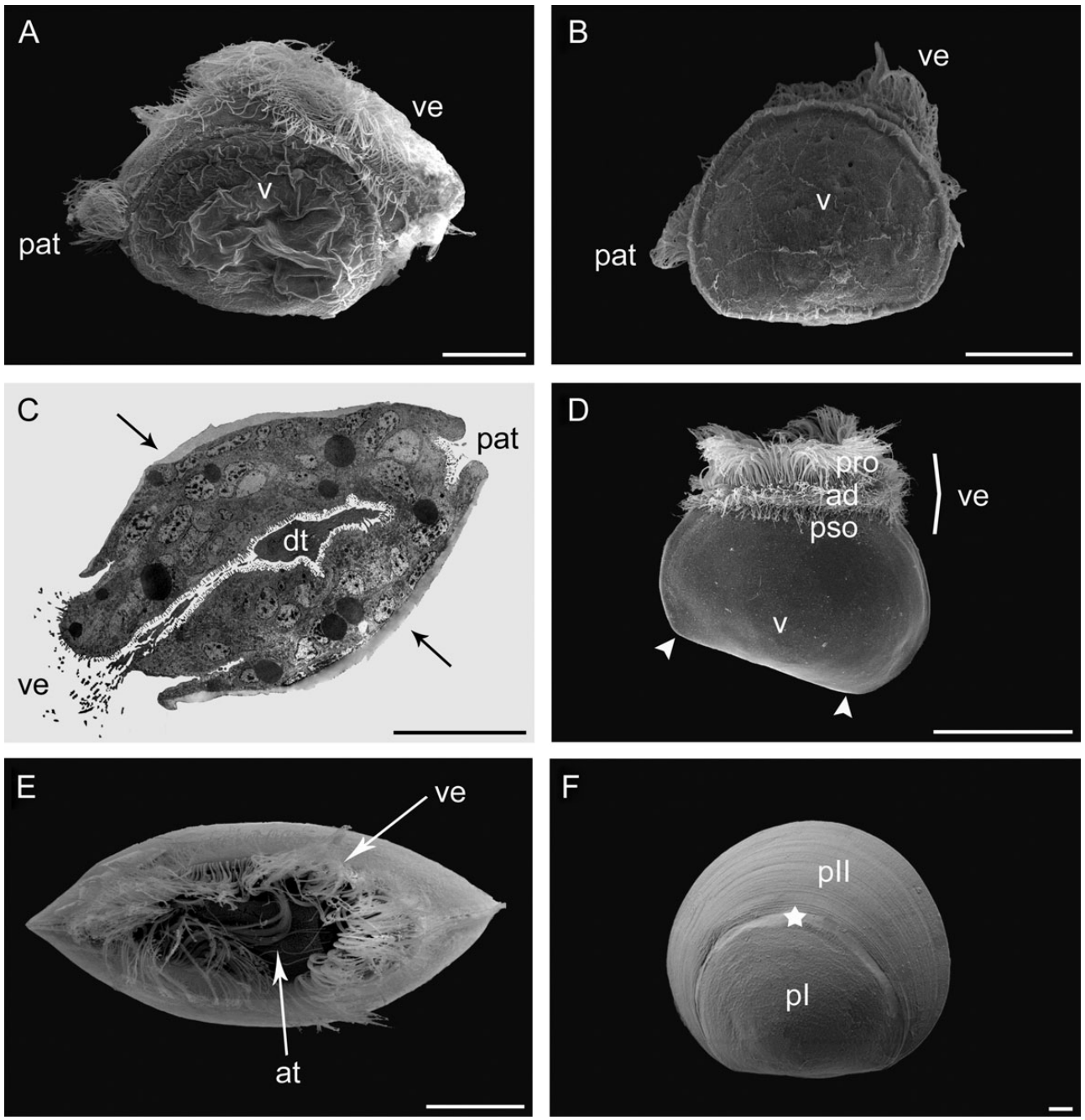

Figure 3. Development of *Ruditapes decussatus*. **A, B, D–F**. Scanning electron microphotographs. **C**. Transmission electron microphotograph. **A**. Late trochophore at $T_0 + 21$ h. The valves cover the entire body and compress the trochophore laterally. The velum is now well developed. **B**. Early D-stage larva at $T_0 + 26$ h. The valves now completely enclose the soft body but still appear uncalcified as suggested by their wrinkled aspect. **C**. Transverse section of a D-larva at $T_0 + 26$ h. The new calcified shell (arrows), which appears grey, is covered by the periostracum. **D**. Early veliger or D-larva at $T_0 + 39$ h, enclosed within the PI. The velum extends between the shell valves and shows three ciliary bands, postoral, adoral with short cilia and inner preoral with long compound cirri. The straight hinge is indicated by arrowheads. **E**. Apical view of D-larva at $T_0 + 39$ h showing velum and apical tuft. **F**. Intermediate veliger stage ($T_0 + 5$d) between D-larva and early umbonate stage showing fully calcified PI and PII, separated by a boundary (star). Abbreviations: at, apical tuft; c, coelom; dt, digestive tract; p, prototroch; pat, postanal tuft; pp, prototrochal pad; t, telotroch; v, valves; ve, velum. Scale bars: **D** = 50 μm; **A, B, E** = 20 μm; **C, F** = 10 μm.

trochophore at $T_0 + 12$ h. Periostracum, as a fine line, appears delineated by arrowheads and attached to the shell gland (curved arrow). Arrows indicate the cilia of the prototroch. **E**. Origin of the periostracum at mantle margin, emanating from secretory T1 cells. The T1 cells in contact with the inner prototrochal cells are characterized by scarce microvilli that are covered by the dense pellicle of periostracum (star). T3 cells are covered by the periostracum and devoid of microvilli. **F**. Trochophore at $T_0 + 17$ h. New shell material (star) is expanding on both sides of first hinge (arrowheads). Bilateral symmetry is now obvious. **G**. Trochophore at $T_0 + 19$ h. The shell material (stars) of the old trochophore spreads out and differentiates into two discrete lobes expanding over the body. The hinge line is now well delineated (arrowheads). **H**. Sagittal section of a late trochophore ($T_0 + 20$ h), showing the open cavity (curved arrows) and the blastopore (straight arrow). Periostracum appears (arrowheads) and continues expanding. Small arrows indicate the cilia of the prototroch. Abbreviations: at, apical tuft; b, blastopore; mc, muscle cells; p, prototroch; pc, prototrochal cells; pp, prototrochal pad; t, telotroch. Scale bars: **A, D** = 30 μm; **B, E** = 5 μm; **C, F–H** = 20 μm.

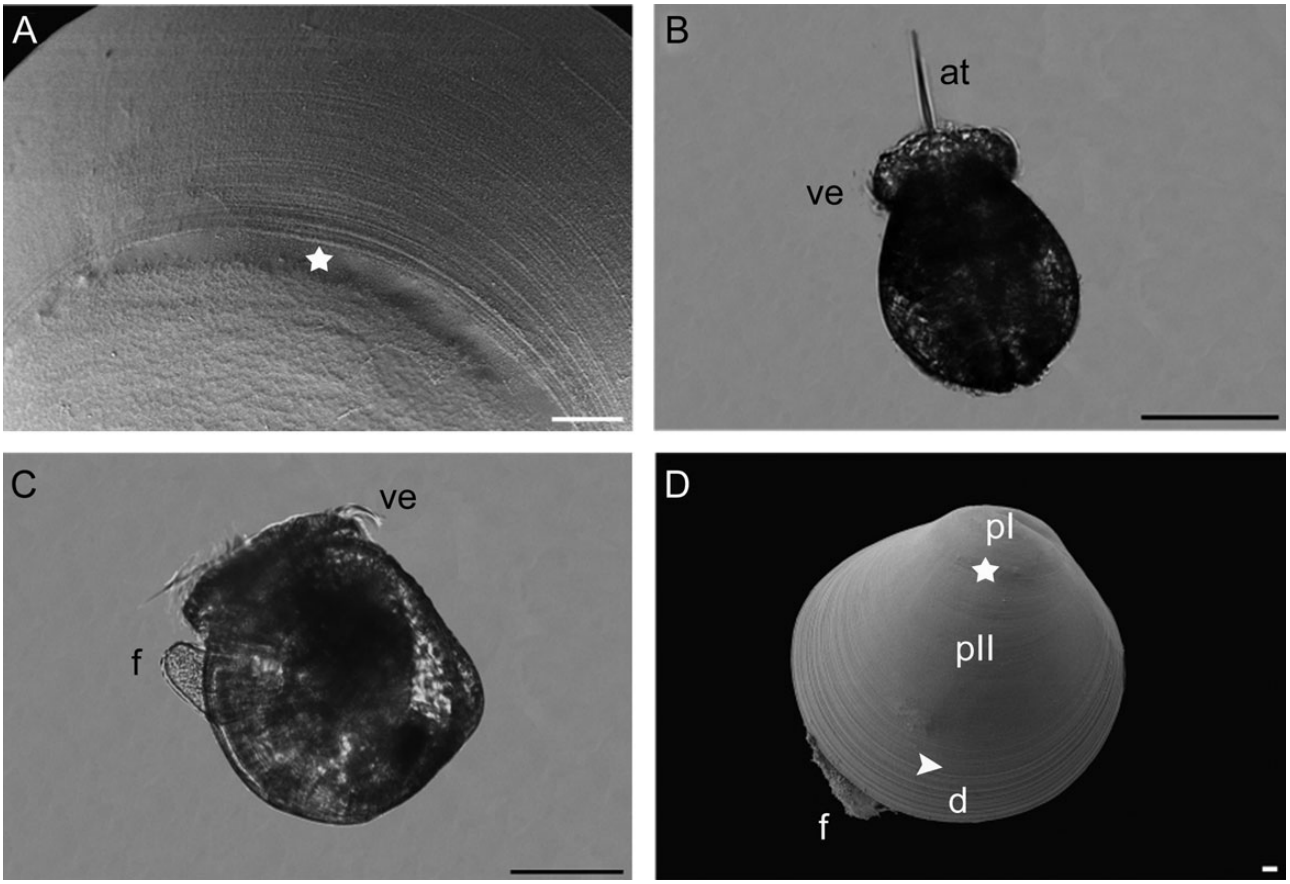

Figure 4. Development of *Ruditapes decussatus*. **A, D**. Scanning electron microphotographs. **B, C**. Optical microphotographs. **A**. Detail of transition (star) between PI (punctate region) and PII (commarginally striated region) in 5-d veliger ($T_0 + 5$ d). **B**. Pediveliger stage ($T_0 + 15$ d), swimming with the velum and apical tuft. **C**. Pediveliger stage ($T_0 + 15$ d) showing velum and foot. **D**. Lateral view of postlarva ($T_0 + 29$d) showing foot. There are two clear demarcations: one (star) between the PI and the PII, and another (arrowhead) between the PII and the dissoconch. Abbreviations: ad, adoral ciliary band; at, apical tuft; d, dissoconch; f, foot; pro, preoral ciliary band; pso, postoral ciliary band; pI, prodissoconch I; pII, prodissoconch II; ve, velum. Scale bars: **B, C** = 100 μm; **A, D** = 10 μm.

Therefore, further investigations are required to ascertain if the pattern in *R. decussatus* is widespread in bivalve larvae.

Currently, our understanding of shell formation in bivalves is based primarily on studies of adults or seed (juveniles), but little is known about the formation of bivalve shells prior to metamorphosis. There are some discrepancies in the descriptions of the differentiation of the bivalve shell during embryonic development. The first studies were based on the process described for gastropods. Using this model, it was shown in *Mytilus galloprovincialis* (Kniprath, 1980) and *Pecten maximus* (Casse, Devauchelle & Le Pennec, 1998) that the invagination needs to close completely before the formation of the shell. However, Mouëza, Gros & Frenkiel (2006) using SEM and TEM proposed an alternative interpretation of the differentiation of the shell in *C. cancellata*, which appears in the trochophore stage as an independent phenomenon. These authors pinpointed that the shell field, which includes both shell- and ligament-secreting cells, only corresponds to the floor of the large depression, does not migrate inward and never undergoes invagination by itself. Later, Cerviño-Otero (2011) demonstrated that the shell differentiation process in *V. pullastra* follows the model proposed by Mouëza, Gros & Frenkiel (2006). In the present study the combined use of SEM and TEM in the venerid *R. decussatus* has confirmed that the shell field appears in the early gastrula, expands between the prototroch and the telotroch, and does not migrate inwards or form an invagination of its own. Consequently, our findings agree with the interpretation of shell differentiation proposed by Mouëza, Gros & Frenkiel (2006). The latter study showed that shell material starts to spread laterally in the early trochophore and that hinge differentiation is obvious at this stage.

In the literature, shell calcification has generally been associated with the formation of the PI. The onset of shell mineralization occurs during the trochophore larval stage (Weiss *et al.*, 2002) and the D-veliger stage already possesses a calcified shell (Bellolio, Lohrmann & Dupre, 1993; Gros, Frenkiel & Mouëza, 1997; Casse, Devauchelle & Le Pennec, 1998; Mouëza, Gros & Frenkiel, 2006; Silberfeld & Gros, 2006; da Costa, Darriba & Martinez-Patino, 2008). In *R. decussatus*, prodissoconch secretion starts during the transition from trochophore to D-larva and, when a typical straight-hinged larva is reached, the calcified shell valves completely enclose the soft body of the embryo. In the early D-larva stage a wrinkled appearance of the valves can be observed when they have completely enclosed the soft body of the embryo. It has been suggested in *Tivela mactroides* that the wrinkled aspect of the shell field is due to organic material that will become calcified at the end of the embryonic development, a few hours prior to the onset of the D-larva stage (Silberfeld & Gros, 2006). The same phenomenon has also been observed in *C. cancellata* and was confirmed by TEM observations of aragonite crystals between the mantle and the periostracum more than 15 h after fertilization (Mouëza, Gros & Frenkiel, 2006). In this study, the wrinkled aspect of the shell could be due to a poor

critical-point drying process and not to uncalcified shells; therefore, further study using other techniques like polarized-light microscopy are needed to detect crystalline calcium carbonate and thus to determine exactly when shells become fully calcified (Weiss *et al*., 2002).

The composition of the ciliary bands in the velum of *R. decussatus* is similar to that of other bivalves and it seems likely that this pattern of velar ciliation is typical of planktotrophic bivalve larvae. Although the inner preoral ring may only be present in some bivalve veligers like *Ostrea chilensis* (Chaparro, Thompson & Emerson, 1999) and *P. maximus* (Cragg, 1989), the main preoral cirri are present in most descriptions of veligers. However, the number of rows that form it is not always clear. An adoral band and postoral ring similar to those observed in *R. decussatus* have been distinguished in many studies of the bivalve velum (Waller, 1981; Cragg, 1989; Bellolio, Lohrmann & Dupre, 1993).

Another common and characteristic structure of numerous species of bivalves is the apical tuft. Tardy & Dongard (1993) described it in *Ruditapes philippinarum* as a set consisting of a central unit, which could function as a mechanoreceptor or chemoreceptor, and a peripheral structure with unknown function. According to investigations in other bivalve species (Cragg, 1989; Gros, Frenkiel & Mouëza, 1997; Mouëza, Gros & Frenkiel, 1999; da Costa, Darriba & Martinez-Patino, 2008), the apical tuft is a structure that appears at the trochophore stage. Although Hodgson & Burke (1988) and Chaparro, Thompson & Emerson (1999) observed in *Chlamys hastata* and *O. chilensis*, respectively, that the apical tuft (or similar structure) remained in the larva until the earliest veliger stage, in this study we can confirm that in *R. decussatus* the apical tuft is present from trochophore to pediveliger stage and, consequently, that it is a permanent structure during larval development until metamorphosis takes place, when it is resorbed with the velum. In addition to its possible sensory functions, we propose that when the pediveliger larva swims actively, the apical tuft could function as a helm.

In *R. decussatus* the surface of the PI showed a punctate pattern and PII bore commarginal growth lines. These features are also found in other venerids, such as *V. pullastra* (Cerviño-Otero, 2011) and *Anomalocardia brasiliana* (Mouëza, Gros & Frenkiel, 1999). According to Weiss *et al*. (2002), the PI is enlarged until the embryo is entirely enfolded and able to close its two valves. Transformation into the motile veliger larva then occurs. The veliger larva enlarges the PI to form PII. After metamorphosis into the postsettlement juvenile stage, the shell is called the dissoconch. The larval PI and PII are preserved during metamorphosis and are integrated into the juvenile and adult shell. Weiss *et al*. (2002), using polarized light microscopy and Raman-imaging spectroscopy, reported that the shell formation process of the PII differs from that of PI. In general, the molluscan larval shell comprises three mineralized layers (Waller, 1981). There is an outer prismatic layer below the periostracum and an inner prismatic layer adjacent to the mantle epithelium. A so-called granular-homogeneous layer with globular structure is embedded between the two prismatic layers. In some cases, the outer prismatic layer is very thin or absent (Weiss *et al*., 2002). This variability, a dependence on the location and age of the shell, and the differences in the formation processes of the PI and PII, may explain the change in the prodissoconch surface.

This is the first study on the embryology and larval development of *R. decussatus*, with special reference to shell differentiation process using SEM and TEM. This study demonstrates that in *R. decussatus* shell formation follows the theory proposed by Mouëza, Gros & Frenkiel (2006). Considering other studies of venerids and Veneroidea, this suggests that shell formation could follow a common pattern throughout the Veneridae and/or Veneroidea.

ACKNOWLEDGEMENTS

This research was funded by Junta Asesora Nacional de Cultivos Marino (JACUMAR). F. da Costa was partly supported by a Fundación Juana de Vega postdoctoral fellowship at IFREMER. We are grateful to the staff of Centro de Cultivos Marinos de Ribadeo-CIMA (Xunta de Galicia). We also thank Suso Méndez, Inés Pazos and Alessandro Benedetti, from the CACTI-University of Vigo, for their helpful assistance in sample preparation for SEM and TEM.

REFERENCES

BELLOLIO, G., LOHRMANN, K. & DUPRE, E. 1993. Larval morphology of the scallop *Argopecten purpuratus* as revealed by scanning electron microscopy. *Veliger*, **36**: 332–342.

CASSE, N., DEVAUCHELLE, N. & LE PENNEC, M. 1998. Embryonic shell formation in the scallop *Pecten maximus* (Linnaeus). *Veliger*, **41**: 133–141.

CERVIÑO-OTERO, A. 2011. *Ciclo reproductivo, cultivo en criadero y en el medio natural de la almeja babosa* Venerupis pullastra *(Montagu, 1803)*. PhD thesis, University of Santiago de Compostela.

CHANLEY, P. E. 1968. Larval development in the class Bivalvia. In: *Proceedings of the Marine Biological Association of India. Symposium on Mollusca*, pp. 475–481.

CHAPARRO, O. R., THOMPSON, R. J. & EMERSON, C. J. 1999. The velar ciliature in the brooded larva of the chilean oyster *Ostrea chilensis* (Philippi, 1845). *Biological Bulletin*, **197**: 104–111.

CRAGG, S. M. 1989. The ciliated rim of the velum of larvae of *Pecten maximus* (Bivalvia: Pectinidae). *Journal of Molluscan Studies*, **55**: 497–508.

CRAGG, S. M. 2006. Development, physiology, behaviour and ecology of scallop larvae. In: *Scallops: biology, ecology and aquaculture* (S. E. shumway & G. J. Parsons, eds), pp. 45–122. Elsevier Science, Amsterdam.

CRAGG, S. M. & CRISP, D. J. 1991. The biology of scallop larvae. In: *Scallops: biology, ecology and aquaculture* (S. E. Shumway, ed.), pp. 75–132. Elsevier Science, Amsterdam.

DA COSTA, F., DARRIBA, S. & MARTINEZ-PATINO, D. 2008. Embryonic and larval development of *Ensis arcuatus* (Jeffreys, 1865) (Bivalvia: Pharidae). *Journal of Molluscan Studies*, **74**: 103–109.

EYSTER, L. S. & MORSE, M. P. 1984. Early shell formation during molluscan embryogenesis, with new studies on the surf clam, *Spisula solidissima*. *American Zoologist*, **24**: 871–882.

FRANZEN, A. 1955. Comparative morphological investigations into the spermiogenesis among Mollusca. *Zoologiska Bidrag fran Uppsala*, **30**: 399–465.

FRANZEN, A. 1956. On spermiogenesis, morphology of the spermatozoon and biology of fertilization among invertebrates. *Zoologiska Bidrag fran Uppsala*, **31**: 355–482.

GROS, O., DUPLESSIS, M. R. & FELBECK, H. 1999. Embryonic development and endosymbiont transmission mode in the symbiotic clam *Lucinoma aequizonata* (Bivalvia: Lucinidae). *Invertebrate Reproduction and Development*, **36**: 93–103.

GROS, O., FRENKIEL, L. & MOUËZA, M. 1997. Embryonic, larval, and post-larval development in the symbiotic clam *Codakia orbicularis* (Bivalvia: Lucinidae). *Invertebrate Biology*, **116**: 86–101.

GWO, J. C., YANG, W. T., SHEU, Y. T. & CHENG, H. Y. 2002. Spermatozoan morphology of four species of bivalve (Heterodonta, Veneridae) from Taiwan. *Tissue and Cell*, **34**: 39–43.

HODGSON, C. A. & BURKE, R. D. 1988. Development and larval morphology of the spiny scallop, *Chlamys hastata*. *Biological Bulletin*, **174**: 303–318.

KNIPRATH, E. 1980. Larval development of the shell and shell gland in *Mytilus* (Bivalvia). *Wilhelm Rouxs Archives of Developmental Biology*, **188**: 201–204.

LINNAEUS, C. 1758. *Systema naturae*. L. Salvvi, Holmiae.

LOOSANOFF, V. L. & DAVIS, H. C. 1963. Rearing of bivalve mollusks. *Advances in Marine Biology*, **1**: 1–136.

LOOSANOFF, V. L., DAVIS, H. C. & CHANLEY, P. E. 1966. Dimensions and shapes of larvae of some marine bivalve mollusks. *Malacologia*, **4**: 351–435.

MOUËZA, M. & FRENKIEL, L. 1995. Ultrastructural study of the spermatozoon in a tropical lucinid bivalve: *Codakia orbicularis* L. *Invertebrate Reproduction and Development*, **27**: 205–211.

MOUËZA, M., GROS, O. & FRENKIEL, L. 1999. Embryonic, larval and postlarval development of the tropical clam, *Anomalocardia brasiliana* (Bivalvia, Veneridae). *Journal of Molluscan Studies*, **65**: 73–88.

MOUËZA, M., GROS, O. & FRENKIEL, L. 2006. Embryonic development and shell differentiation in *Chione cancellata* (Bivalvia, Veneridae): an ultrastructural analysis. *Invertebrate Biology*, **125**: 21–33.

OCKELMANN, K. W. 1965. Developmental Types in Marine Bivalves and their Distribution along the Atlantic Coast of Europe. In: *Proceeding of the First European Malacological Congress* (L. R. Cox & J. F. Peake, eds), pp. 25–35. Conchological Society of Great Britain and Ireland and the Malacological Society of London, London.

SILBERFELD, T. & GROS, O. 2006. Embryonic development of the tropical bivalve *Tivela mactroides* (Born, 1778) (Veneridae: subfamily Meretricinae): a SEM study. *Cahiers de Biologie Marine*, **47**: 243–251.

TARDY, J. & DONGARD, S. 1993. Le complexe apical de la véligère de *Ruditapes philippinarum* (Adams et Reeve, 1850) Mollusque Bivalve Vénéridé. *Comptes Rendus de l'Académie des Sciences. Série III, Sciences de la Vie (Paris)*, **316**: 177–184.

VELA, J. M. & MORENO, O. 2005. Pérfil bio-ecológico de la almeja fina (*Tapes decussatus* (Linneus, 1758)). In: *Acuicultura, pesca y marisqueo en el Golfo de Cádiz* (J. Morales, A. J. Mata & A. Rodríguez, eds), pp. 641–662. Consejería de Agricultura y Pesca, Junta de Andalucía, Sevilla.

VERDONK, N. H. & VAN DEN BIGGELAAR, J. A. M. 1983. Early development and the formation of germ layers. In: *The Mollusca, vol. 3. Development* (N. H. Verdonk, J. A. M. Van den Biggelaar & A. S. Tompa, eds), pp. 91–122. Academic Press, New York.

WALLER, T. R. 1981. Functional morphology and development of veliger larvae of the European oyster, *Ostrea edulis* Linné. *Smithsonian Contributions to Zoology*, **328**: 1–70.

WEISS, I. M., TUROSS, N., ADDADI, L. & WEINER, S. 2002. Mollusc larval shell formation: Amorphous calcium carbonate is a precursor phase for aragonite. *Journal of Experimental Zoology*, **293**: 478–491.